Grayscale lithography process study applied to zero-gap microlenses for sub 2μm CMOS image sensors

S. Audran, Jérôme Vaillant, V. Farys, F. Hirigoyen, E. Huss, B. Mortini, C. Cowache, L. Berthier, E. Mortini, J. Fantuz, et al.

Grayscale lithography process study applied to zero-gap microlenses for sub 2µm CMOS image sensors

S. Audran*[a], J. Vaillant, V. Farys[a], F. Hirigoyen[a], E. Huss[a], B. Mortini[a], C. Cowache[a], L. Berthier[a], E. Mortini[a], J. Fantuz[a], O. Arnaud[a], L. Depoyan[a], F. Sundermann[a], C. Baron[a], J-P. Reynard[a]
[a]STMicroelectronics, 850 rue Jean Monnet, 38926 Crolles Cedex, France

ABSTRACT

Microlens arrays are used on CMOS image sensors to focus incident light onto the appropriate photodiode and thus improve the device quantum efficiency. As the pixel size shrinks, the fill factor of the sensor (i.e. ratio of the photosensitive area to the total pixel area) decreases and one way to compensate this loss of sensibility is to improve the microlens photon collection efficiency. This can be achieved by developing zero-gap microlens processes. One elegant solution to pattern zero-gap microlenses is to use a grayscale reticle with varying optical densities which locally modulate the UV light intensity, allowing the creation of continuous relief structure in the resist layer after development. Contrary to conventional lithography for which high resist contrast is appreciated to achieve straight resist pattern profiles, grayscale lithography requires smooth resist contrast curve. In this study we demonstrate the efficiency of grayscale lithography to generate sub-2µm diameter microlens with a positive-tone photoresist. We also show that this technique is resist and process (film thickness, development normality and exposure conditions) dependent. Under the best conditions, spherical zero-gap microlenses as well as aspherical and off-axis microlenses, which are impossible to obtain with the conventional reflow method, were obtained with satisfying process latitude.

Keywords: Grayscale, microlens, halftoning, zero-gap, photoresist, contrast curve

1. INTRODUCTION

Microlens arrays are used in CMOS image sensors to focus incident light onto the photodiode and thus improve the device quantum efficiency. A common and well-know method to manufacture refractive microlens is the thermal reflow technique[1]. This method consists in forming resist patterns using a conventional lithographic process step with a binary mask and then melting the resist dots so that surface tension pushes them to adopt spherical form. One limitation of this technique is that a minimum space between microlenses (around 300nm for I-line lithography) has to be kept to prevent lens merging during the melting step. Indeed lens merging leads to a change of microlens height and curvature radius and thus degrades their optical performance. As the pixel size shrinks, the fill factor of the sensor (i.e. ratio of the photosensitive area to the total pixel area) decreases and one way to compensate this loss of sensibility is to improve the microlens photon collection efficiency. This can be achieved by developing zero-gap microlens processes.

One classical and simple technique to obtain zero-gap microlenses is to keep a binary mask and perform a double lithographic step[2]. However this process leads to two series of microlenses that do not present exactly the same morphological characteristics and thus the same optical performances. Moreover this double-step process is time consuming and more subject to alignment errors than single step process. An elegant solution to perform zero-gap microlenses is the use of a grayscale mask with varying optical densities which locally modulate the UV light intensity, allowing the creation of continuous relief structure in the resist layer after development. The main advantage of this technique is to reduce the process cycle by using a single mask and thus come back to a single lithographic step. In the same time it enables to improve overlay. From a performance point of view, another advantage of this method is to offer the possibility to design non-conventional shapes such as aspherical or off-axis microlenses that can not be obtained with the conventional melting technique.

There are different types of grayscale masks. The High Energy Beam Sensitive (HEBS) mask is made of a specific glass (glass matrix in which silver ions have been incorporated) that darkens upon electron beam exposure: the more electrons

*Stephanie.audran@st.com; phone +33 4 76 38 32 01; fax +33 4 76 92 68 14

dosage the darkest the glass becomes [3,4].The Laser Direct Write (LDW) mask is made the same way as the HEBS mask except that pattern writing on the mask is based on erasure of opaque silver particles by laser exposure heat. Another common type of grayscale mask that will be discussed in this paper is the chrome-on-quartz mask. As in standard binary mask, the chrome makes up the dark field but such grayscale masks employ sub resolution regions of chrome that functions like opaque particles. Chrome-on-quartz masks are advantageous because standard binary mask fabrication techniques can be easily adapted to generate these masks.

The variation in transmission of a chrome-on-quartz reticule can be realized in different ways. The most elementary technique, the halftoning method, consists in dividing a matrix or a pixel (which corresponds for example to the size of a microlens) into fixed cells whose size corresponds to the minimum chrome dot size. At each point of the pixel, only the presence or the absence of the chrome dot is specified and this is the global arrangement of these dots within the pixel that will give a halftoned image. Strictly speaking there are no discrete gray levels in the halftoning method. More advanced techniques such as the Pulse-Width Modulation (PWM) and the Pulse-Frequency Modulation or Pulse Density Modulation (PDM) methods enable to add one degree of liberty [5]. Indeed the PWM consists in dividing the global pixel in cells of fixed size and varying the chrome dot size within the cell to generate the different gray levels; whereas the PDM method consists in keeping the chrome dot size constant and making the cell pitch varies. Finally more recent methods relay on adjusting both the shape and the position of the chrome dot which gives an extra freedom to control the design accuracy [6].

In this paper we will focus on the use of the halftoning grayscale technique to generate sub 2µm zero-gap microlenses. After a short description of the experimental conditions, we first expose the grayscale principle, the different ways of dots arrangements we have considered and the resist requirements associated to grayscale photolithography. Then we explain the different steps required to generate the grayscale mask. Finally we evaluate the microlens process latitude obtained with a grayscale technique.

2. EXPERIMENTAL

Microlenses were fabricated using I-line positive photoresists. Microlens photoresist was spin-coated on 12 inch silicon wafers and soft baked in a temperature range of 90-100°C during 90s. The wafers were then exposed on an I-line stepper (NA=0.6; σ=0.35) with a dose range of 100-450 mJ/cm^2 and developed in a basic aqueous solution for 80s. At the end of this step we obtain microlens that are not stabilized.
The final process step consists in hard baking the microlenses on a hot plate at a specific temperature, between 150°C-230°C for 3-5 min. During this step resist crosslinking occurs leading to a highly stable three-dimensional network.
The measurements of microlens profiles and remaining thickness of specific patterns used to build the calibration curve were carried out by Atomic Force Microscopy (AFM). Microlens topviews and cross sections were respectively characterized on SEMCD and HRSEM tools.

3. GRAYSCALE PRINCIPLE AND RESIST REQUIREMENTS

3.1 Grayscale principle

The principle of this technique is to modulate the incident light intensity arriving at the surface of the resist layer by modulating the transmission of the chrome-on-quartz mask (figure1). This is obtained by creating either arrays of holes in a dark-field reticle (chrome mask) or arrays of opaque islands on a bright-field mask. One condition to avoid the transfer of the dot in the resist and obtain a continuous relief structure after development is to use dot whose size is smaller than the stepper resolution.

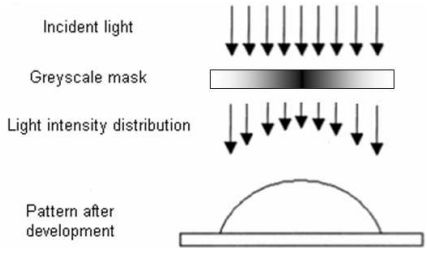

Figure 1: Principle of the grayscale technique

As discussed in the introduction, in this study, we use the halftoning method to generate the grayscale patterns. There are different ways of arranging fixed-size dots on a regular matrix. The three algorithms that are commonly used to code the halftone image are the random dithering, the ordered dithering and the error diffusion dithering also called Floyd-Steinberg dithering [7, 8]. All of these algorithms will be evaluated in part 4.

Another important point that must be fulfilled when we form microlenses with grayscale lithography process is that the shape obtained in the resist after development (in our case spherical cap shape) must stay unchanged during the subsequent process steps (i.e. crosslinking hard bake steps).

3.2 Resist requirements

Photoresists used to manufacture microlenses for CMOS Imagers must fulfill two important properties which are a high refractive index (around 1.6) and a high thermal and chemical stability. Indeed at the end of their process microlenses are becoming an entire part of the chip and therefore they should withstand not only the thermal budget associated to the operations that follows the microlens formation (chip packaging) but also the external constraints (UV exposition, thermal budget…) that the chip will undergo during its life time. High levels of stability are achieved by using specific polymer structures that crosslink under thermal activation. This means that once the mirolenses are formed, a hard bake step is added to the standard photolithographic process in order to stabilize the resist.

When using a grayscale mask to form microlenses, two additional requirements should be considered. The first one is the use of non-flow resist material. Indeed contrary to the reflow method, where the microlens spherical shape is obtained during the resist melting step, grayscale microlenses shape is defined during the development step. As described above, subsequent hard bake steps are still necessary to stabilize the resist but the microlens shape must stay unchanged during these high temperature bakes, otherwise the final microlens shape will not be faithful to the original microlens shape designed at the mask level. This means that we need to crosslink the resist without melting it: this can be realized if the resist glass transition temperature T_g is superior to its crosslinking temperature. The second important condition is the use of low contrast photoresists such as those based on diazonaphtoquinone (DNQ) photosensitizers. Indeed to achieve continuous relief profile in the resist under varying transmission, the resist thickness change response versus dose must be very smooth. In this condition the photoresist thickness after development will be proportional to the local exposure.

As we will see in section 4, there is a strong correlation between the resist contrast curve and the mask design.

4. CALIBRATION CURVE FOR GRAYSCALE MASK GENERATION

4.1 Methodology

The principle used to design the microlens grayscale mask is the following:

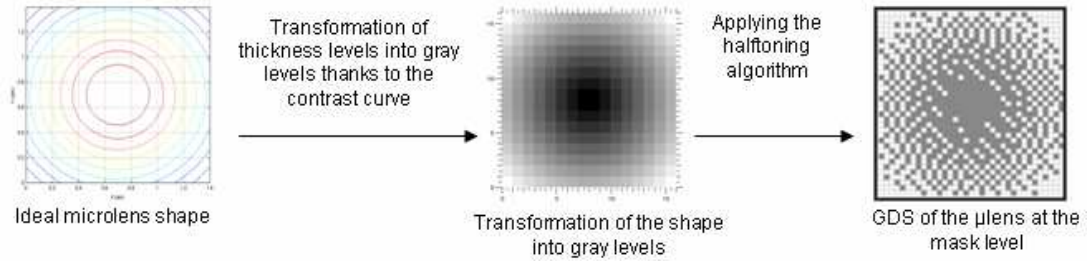

Figure 2: Methodology to design the grayscale mask

We start with the three dimension representation of the ideal microlens that we want to transfer at the resist level. Then thanks to a calibration curve that gives the remaining resist thickness obtained after development as a function of the gray levels, the 3D ideal shape is transformed into gray levels. Finally, once the right algorithm has been chosen, we apply the halftoning algorithm to the gray level pattern to obtain the design that must be realized at the mask level.

Therefore the measurement of the resist calibration curve (section 4.3) and the choice of the optimal halftoning algorithm (section 4.4) are the mandatory steps before the coding of the grayscale mask.

As we will see in next section, the choice of the resist is also a very important point.

4.2 Resist candidates

We started the study with three different I-line resists from three different suppliers. All resist candidates are positive tone photoresists that fulfill the requirements described in section 3.2. They principally differentiate each other by the shape of their contrast curve. The contrast curve of each resist is depicted in figure 3.

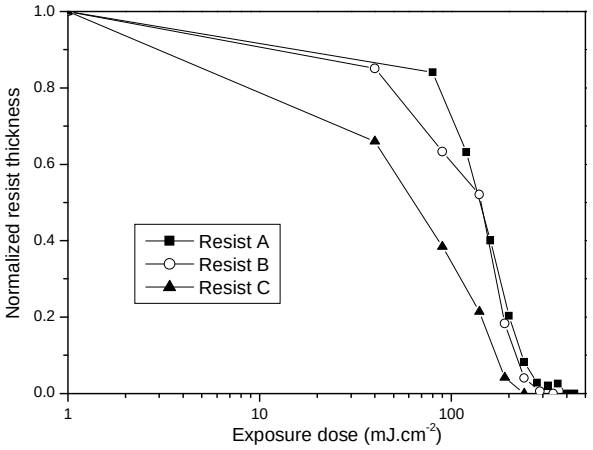

Figure 3: Contrast curves of the three resist candidates

This graph shows that the contrast curves of resist A and B are quite similar. Moreover their slope is much steeper than that of resist C. This indicates that resist C should be more adapted to grayscale technology than the two other resists.

These contrast curves correspond to one set of process conditions. If we change one process condition like the developer nature (figure 4(a)) or if we introduce an additional step like a Post Exposure Bake (PEB) (figure 4(b)) it directly impacts the shape of the contrast curve. In this example both developers have a very close TMAH concentration but we see that the resist sensitivity is increased due to the additive influence. On the other hand, resist sensitivity can be strongly reduced by adding a PEB step. Indeed we start to partially crosslink the polymer matrix during this step and consequently we modify the resist dissolution rate in the developer. As a consequence these two process parameters can be used to adjust precisely the slope of the resist contrast curve.

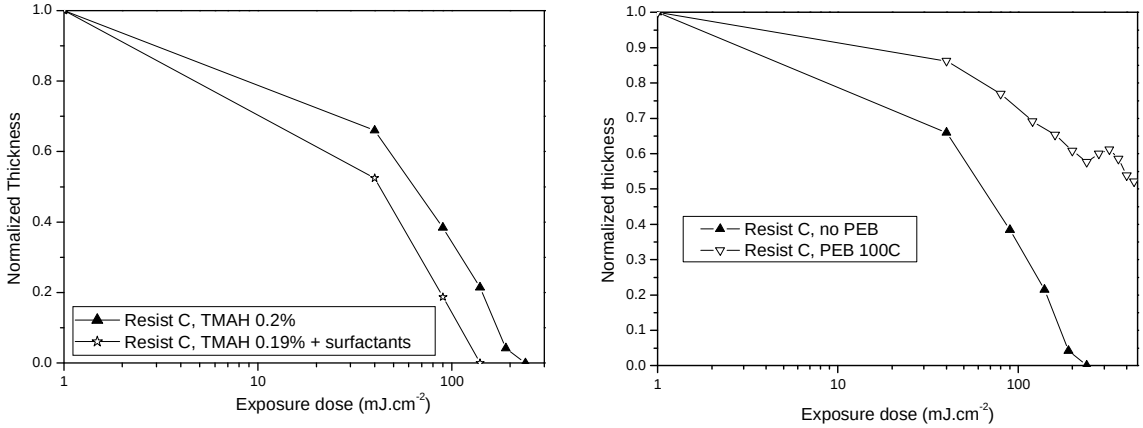

(a) (b)

Figure 4: Effect of developer nature (a) and the addition of a PEB step (b) on the resist C contrast curve

4.3 Resist selection

In order to see which resist is the more appropriate to grayscale photolithography, we need to know the relationship between the residual resist film thickness and the dot density at the mask level. For that purpose, a progressively stepped linear gray scale with ten different gray levels has been designed on a mask (figure 5) and printed using the three resists. Then the remaining resist thickness has been measured by AFM. The grayscale pattern has been coded in three different ways using the three different halftoning algorithms described in part 3.1: the ordered, random and the error diffusion algorithms.

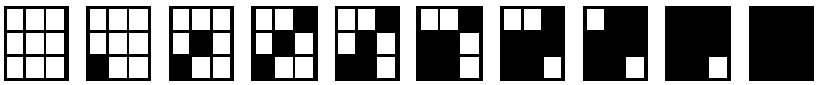

Figure 5: Example of linear gray scale structure coded with the ordered algorithm

Figure 6(a) shows the contrast curve of resist C obtained with the three different algorithms. Figure 6(b) compares the contrast curve of the three resist candidates obtained with the error diffusion algorithm. For each resist, the contrast curve has been measured at the dose for which the ten gray levels were printed.

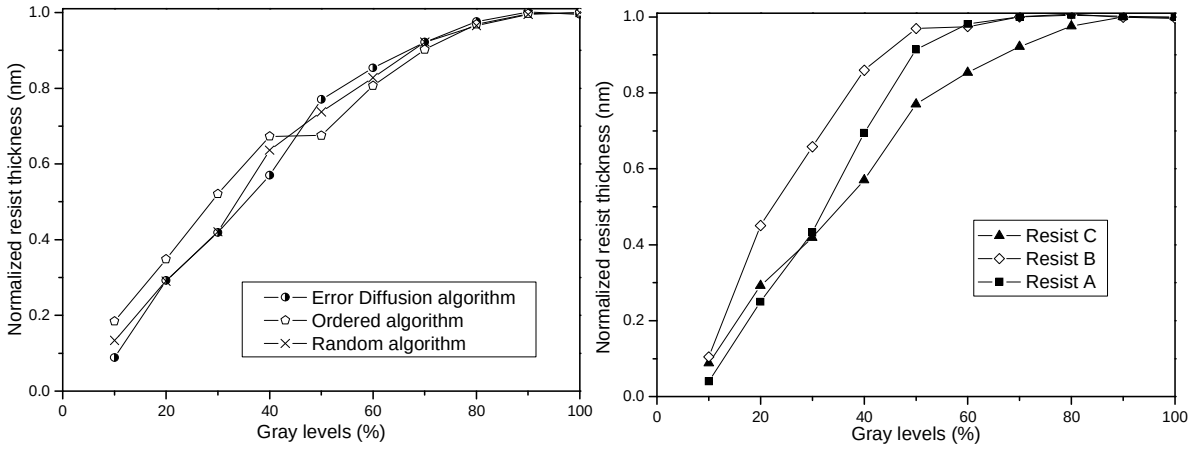

Figure 6: (a) Contrast curves of resist C obtained with three different algorithms; (b) Comparison of the contrast curve of the three resist candidates obtained with the error diffusion algorithm

Figure 6a shows that the contrast curves of the resist C obtained with the three different halftoning algorithms are equivalent. Figure 6b shows that whatever the resist, we obtain a convex contrast curve. We also see that the sensibility of the resist C to the darkest gray levels is better and the slope of its contrast curve is slightly less steep compared to the two other resists. This result suggests that the controllability of resist C will be better. That's why the rest of the study has been conducting focusing on resist C performance.

The calibration curve obtained in this section enables to correlate the remaining resist thickness to the gray levels. Next part will concentrate on the choice of the best halftoning algorithm.

4.4 Choice of the optimal halftoning algorithm

Using the calibration curve of resist C, different microlens shapes have been coded on a grayscale mask with the three different algorithms: the ordered, the random and the error diffusion one. Wafers coated with resist C have then been exposed with this mask. The resulting microlenses were characterized by SEMCD, HRSEM and AFM.

Figure 7 shows the result obtained with the random algorithm. Microlenses present a random shape that is not uniform along the matrix and that do not correspond to the hemispherical shape coded at the mask level.

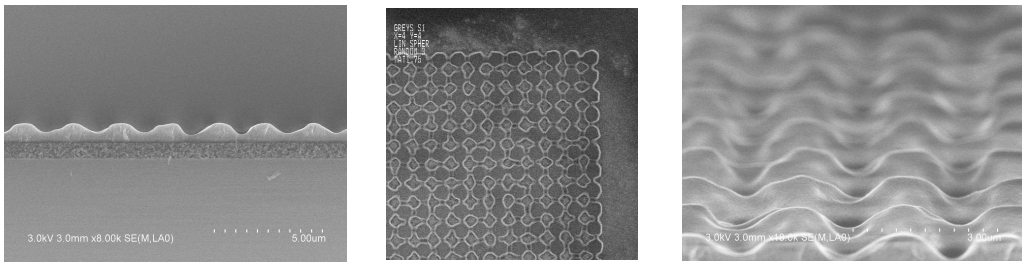

Figure 7: SEMCD pictures of 2.2 µm microlenses obtained at the wafer level with the random algorithm

Figure 8 presents the results of four spherical microlenses designed with three different heights and coded with the ordered algorithm. We see that the highest microlenses are well formed whereas the smallest one has a flat profile.

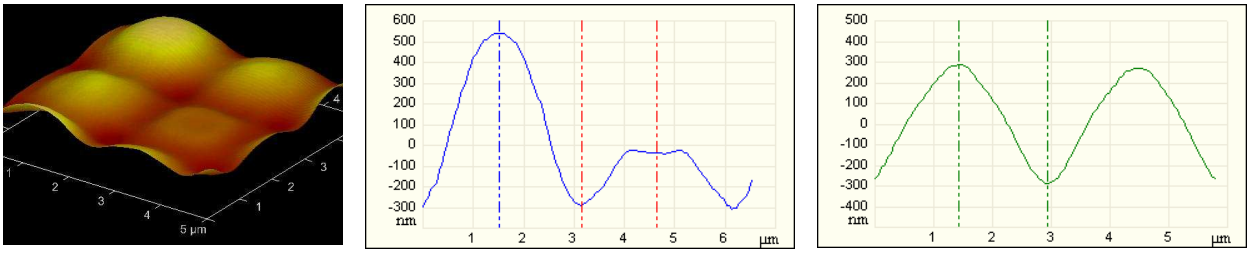

Figure 8: AFM scan and diagonal profiles of 2.2 µm spherical microlenses obtained at the wafer level with the ordered algorithm

Finally figure 9 shows the same pattern coded with the error diffusion algorithm. In this case, microlenses are rounded whatever the height which shows that this algorithm is more suitable than the others.

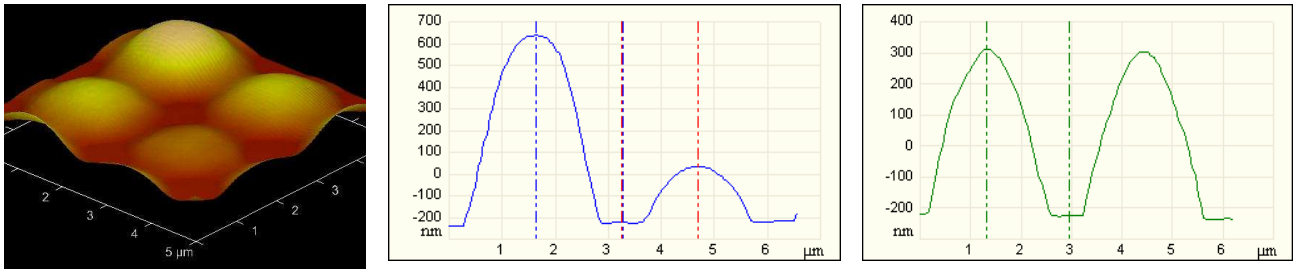

Figure 9: AFM scan and diagonal profiles of 2.2µm spherical microlenses obtained at the wafer level with the error diffusion algorithm

These results show that the error diffusion algorithm enables a better controllability of the pattern transfer into the resist. As a consequence we select this algorithm as our reference for the rest of the study.

4.5 Importance of the calibration curve

Figure 10 presents SEMCD tilted views of spherical microlenses coded with the halftoning algorithm and a contrast curve that fits the experimental calibration curve of the resist C. As we can see nice and repeatable microlenses are obtained after development. AFM scans of these microlenses are displayed in figure 11 (a), as well as AFM of more exotic shapes like off-axis microlenses (figure 11(b)) and aspherical microlenses (figure 11(c)).

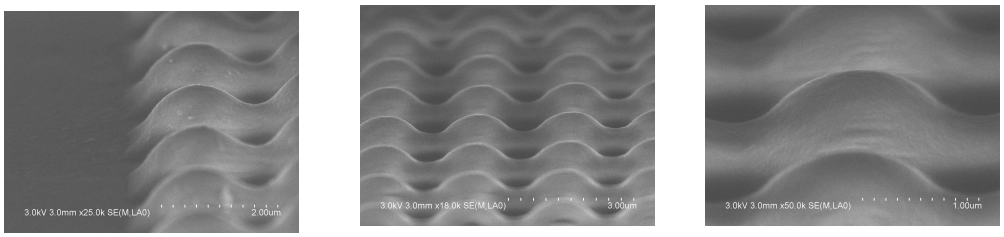

Figure 10: SEMCD cross-section of 2.2µm spherical microlenses obtained with resist C and error diffusion algorithm

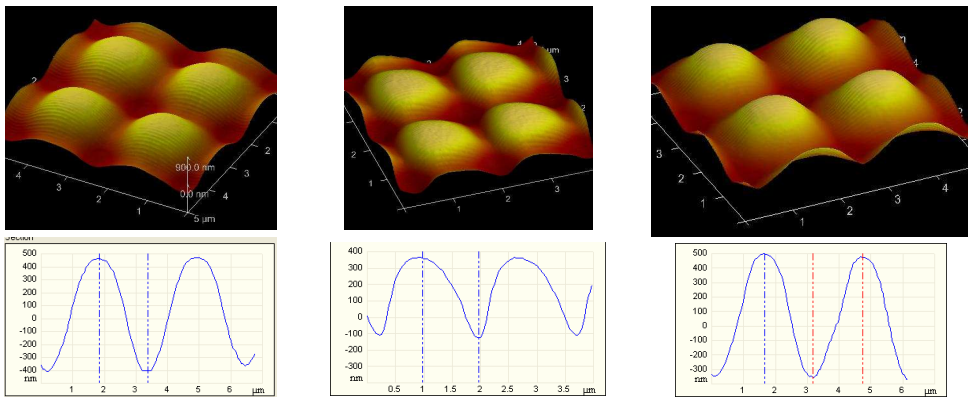

(a) (b) (c)

Figure 11: AFM characterization of (a) 2.2µm spherical microlenses, (b) 1.75µm off-axis microlenses and (c) 2.2µm aspherical microlenses

These results show that once the right calibration curve and the right algorithm have been chosen, the grayscale technique enables to print different microlens shapes on a same wafer in one single exposure, which is absolutely not possible with the standard reflow technique.

However, if the contrast curve coded in the grayscale mask does not perfectly fit the calibration curve obtained from the linear gray scale structure, it directly impacts the shape obtained at the wafer level as displayed on figure 12 where flat microlenses are obtained instead of spherical one.

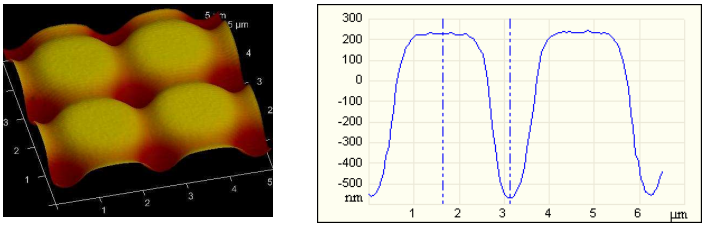

Figure 12: AFM characterization of 2.2µm microlenses coded with a contrast curve that does not perfectly fits the calibration curve of the resist

To conclude, the choice of the right resist candidate (low contrast and good response to a maximum of gray levels) and the right algorithm are the first steps to achieve. Then in order to facilitate the proper calibration of resist removal, a calibration curve correlating the remaining resist thickness versus the gray levels has to be obtained. This curve is indispensable to the right coding of the halftoning structure and the faithful transfer of the targeted structure into the resist.

Now that we have found a working point to generate grayscale microlenses, we will study in the next section the latitude of this process.

5. MICROLENS PROCESS LATITUDE WITH GRAYSCALE TECHNIQUE

5.1 Ideal targeted microlens shape

The ideal shape designed at the mask level is represented on figure 13. In order to collect the maximum of photons at the surface of the Imagers, the microlenses need to present a square base with a zero gap between each other. In this condition the covering of the pixel is maximum and the efficiency of the microlenses optimal. Another important point is the curvature radius of the microlens. This must be uniform in horizontal and diagonal directions in order achieve one single focalization point closed to the photodiode level.

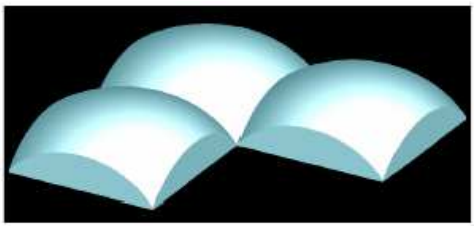

Figure 13: Ideal square-based zero-gap microlenses coded at the mask level

5.2 Influence of resist thickness

In this part we have studied the effect of resist thickness variations on the final microlens shape. Two wafers have been coated at a spin speed of 1500rpm and 1300rpm and exposed at a same dose of 200mJ.cm^{-2}. SEMCD top views and AFM profiles are displayed on figure 14.

As expected, microlenses coated at 1300rpm are higher than that coated at 1500rpm and the microlens profile comparison (Figure 14(c)) suggests that the two series of microlenses have a different curvature radius. That's why one grayscale mask design corresponds to a specific resist thickness, the one that has been used to obtain the calibration curve.

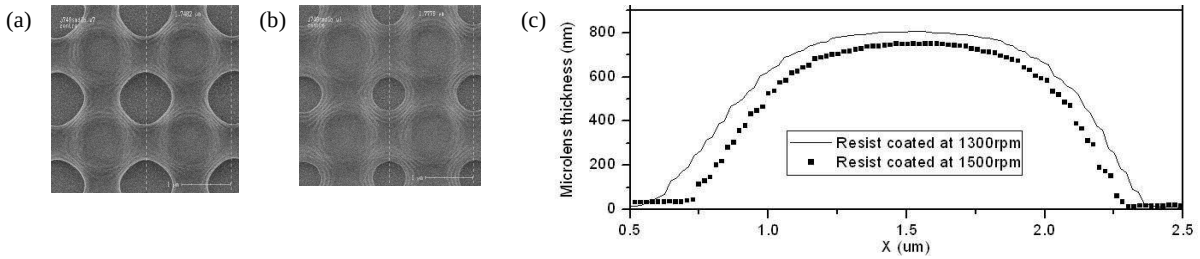

Figure 14: SEMCD top views of 1.75µm grayscale microlenses obtained (a) with a spin speed of 1500rpm and (b) a spin speed of 1300rpm and (c) the comparison of both diagonal AFM profiles

5.3 Effect of dose and focus

In this part we study the effect of dose and focus variations on microlens obtained with the grayscale mask. Figure 15 displays the evolution of microlens shape as a function of dose, figure 16 the evolution of microlens profile as a function of focus.

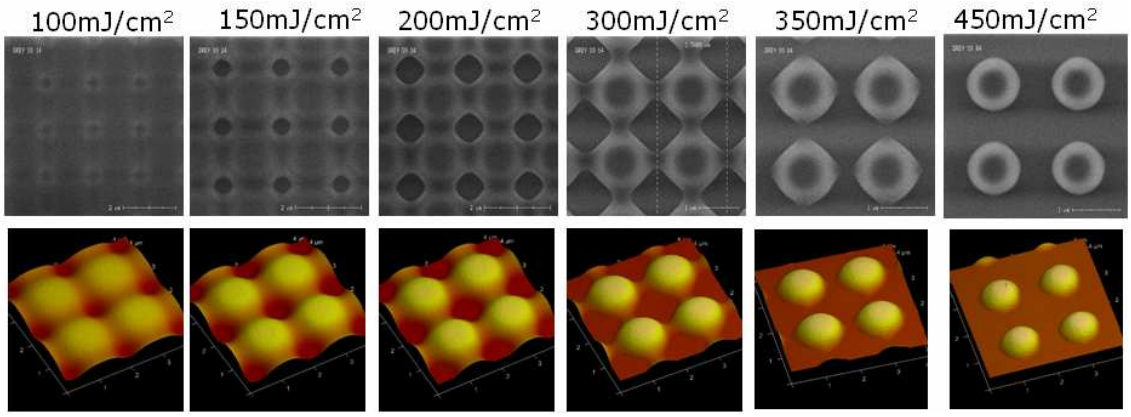

Figure 15: Effect of exposure dose on 1.75µm microlens shape (for a given focus)

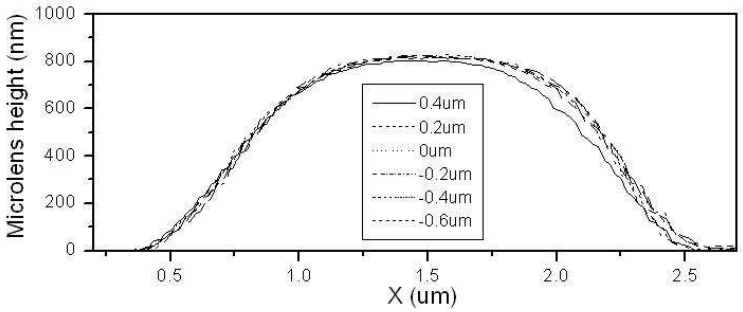

Figure 16: Effect of focus on 1.75µm microlens profile (for a given dose)

Figure 15 shows that as dose increases, the overlap between microlenses in X and Y direction disappears to give non-zero-gap microlenses. At the same time the optical dead area at the corner of four microlenses increases. This phenomenon leads to a loss of microlens photon collection efficiency. The optimal dose (zero gap microlenses and minimum dead area) is between 100mJ.cm^{-2} and 150mJ.cm^{-2}. As a consequence, for a given resist thickness, the optimized microlens shape is associated to a specific and single dose.

On the contrary figure 16 shows that the DOF associated to the microlens obtained with a grayscale mask is relatively wide since we did not detect any specific effect when the focus leveling varies from 0.4µm to -0.6µm.

5.4 Effect of developer normality

The objective of this part is to evaluate the effect of developer normality on the microlens shape at a given resist thickness and a fixed dose. Figure 17 displays SEMCD top views of microlenses obtained with two different developer normalities and equivalent doses. Figure 18 shows the comparison in horizontal and diagonal direction of the microlens profiles obtained with the two developer normality at a dose of 150mJ.cm^{-2}.

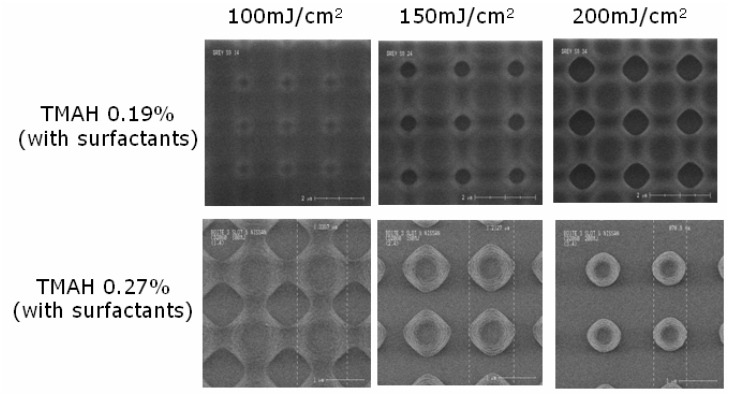

Figure 17: Comparison of 1.75µm SEMCD microlens top views obtained with a developer normality of TMAH 0.19% and a developer normality of TMAH 0.27%

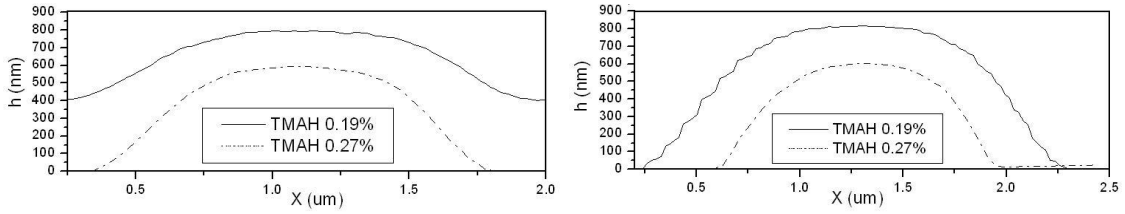

Figure 18: Comparison of AFM profiles of 1.75µm microlenses obtained with both developer normality (with surfactants): (a) horizontal profiles (b) diagonal profiles

These results show that increasing the developer normality of almost 0.1% has a similar effect than increasing the dose of 200mJ.cm^{-2}. Figure 18 confirms that the developer normality has a significant impact on the microlens profile both in term of height and curvature radius.

To conclude on the latitude of the grayscale technique, we can say that one grayscale mask is specific to one resist associated to one specific process i.e. a given combination of resist thickness, dose and developer. Any change of one of these parameters will directly impact the shape of the microlenses transfer at the resist level.

5.5 Effect of hard bake temperature

As explained in part 2.2, one specific requirement associated with grayscale technology is the use of non-flow microlens resist type. Indeed to faithfully transfer the microlens shape from the mask to the resist level one important thing is to minimize the change of microlens shape induced by the final hard bake steps. As previously explained these final bakes are used to stabilize i.e. crosslink the resist and thus are an integral part of the microlens process.

Figure 19 shows the evolution of microlens shape after a final hard bake at 200°C. Even if the resist used (resist C) belongs to the category of non-flow type material, we clearly see that some resist melting occurs during the hard bake step and has for effect to significantly change the microlens shape which must be avoided.

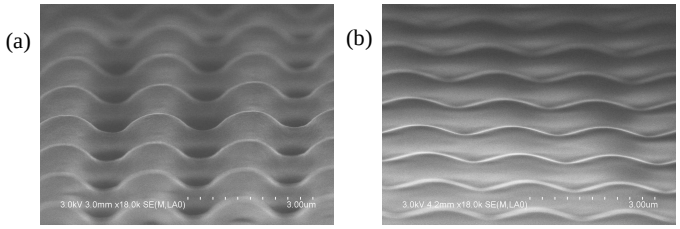

Figure 19: Comparison of SEM tilted view of microlenses obtained (a) after development and ((b) after a final hard bake step at 200°C

By optimizing the hard bake temperature it is possible to efficiently limit the melting of the resist during the hard bake step. Indeed figure 20 shows that by decreasing the HB temperature of 20°C, the change of microlens profile before and after HB steps is clearly reduced.

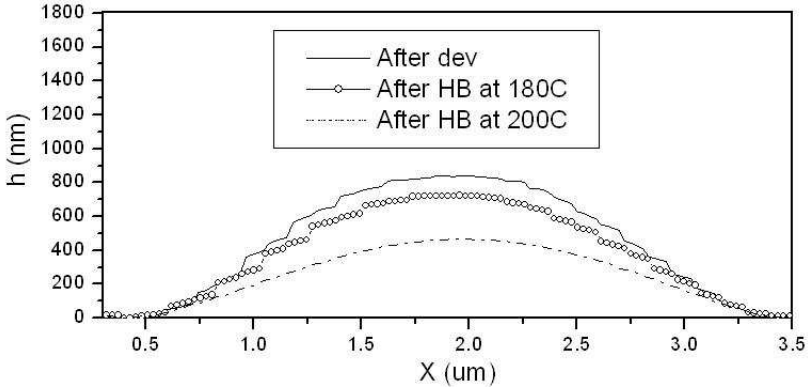

Figure 20: Comparison of AFM profiles of 1.75µm microlens obtained after development and two different hard bake temperatures

6. CONCLUSION

In this study we have demonstrated the efficiency of grayscale lithography to generate sub-2µm diameter microlens with a positive-tone photoresist which is then crosslinked during a final HB step. We demonstrate that this technique is resist and process (film thickness, development normality…) dependent.

Under the best conditions spherical zero-gap microlenses as well as aspherical and off-axis microlenses, which are impossible to obtain with the conventional reflow method, were obtained with satisfying process latitude (DOF>1µm, good EL).

This works outlines the clear benefits of grayscale lithography applied to zero-gap microlens for CMOS imagers but also points out some of its difficulties, such as the strong correlation between mask design and resist choice as well as process conditions (developer chemistry, film thickness and bake temperature).

REFERENCES

[1] Audran, S., Faure, B., Mortini, B., Aumont, C., Tiron, R., Zinck, C., Sanchez, Y., Fellous, C., Regolini, J., Reynard, J.P., Schlatter, G. and Hadziioannou, G., “Study of dynamical formation and shape of microlenses formed by the reflow method”, Proc. SPIE 6153, 61534D (2006)

[2] Lee, S.U., Park, J.L, Choi, J.S. and Lee, J.G., “The fabrication process and characteristics of light loss free zero-space microlenses for CMOS image sensor”, Proc. SPIE 5754, pp. 1241-1248 (2005)

[3] Dillon, T., Zablocki, M., Murakowski, J. and Prather, D., “Processing and modeling optimization for grayscale lithography”, Proc. SPIE 6923, pp. 69233B-69233B-13 (2008)

[4] Dykes, J.M. and Chapman, G.H, “Enhanced laser-writing techniques for bi-metallic grayscale photomasks”, Proc. SPIE 7488 (2009)

[5] Henke, W., Hoppe, W. and Quenzer H-J., “Simulation and process design of gray-tone lithography for the fabrication of arbitrarily shaped surfaces”, Jpn. J. Appl. Phys. 33, 6809-6815 (1994)

[6] Su, J., Du, J., Yao, J., Gao, F., Guo, Y. and Cui, Z., “A new method to design half-tone mask for the fabrication of continuous micro relief structure”, Proc. SPIE 3680 (1999)

[7] Bayer, B.E., "An optimum method for two-level rendition of continuous-tone pictures". IEEE International Conference on Communications 1, 11–15 (1973)

[8] Floyd, R.W. and Steinberg, L., “An adaptive algorithm for spatial grey scale”, Proc. of the Society of Information Display 17, 75–77 (1976).